

Developing a genetic signature to predict drug response in ovarian cancer

SUPPLEMENTARY MATERIALS

JC-1

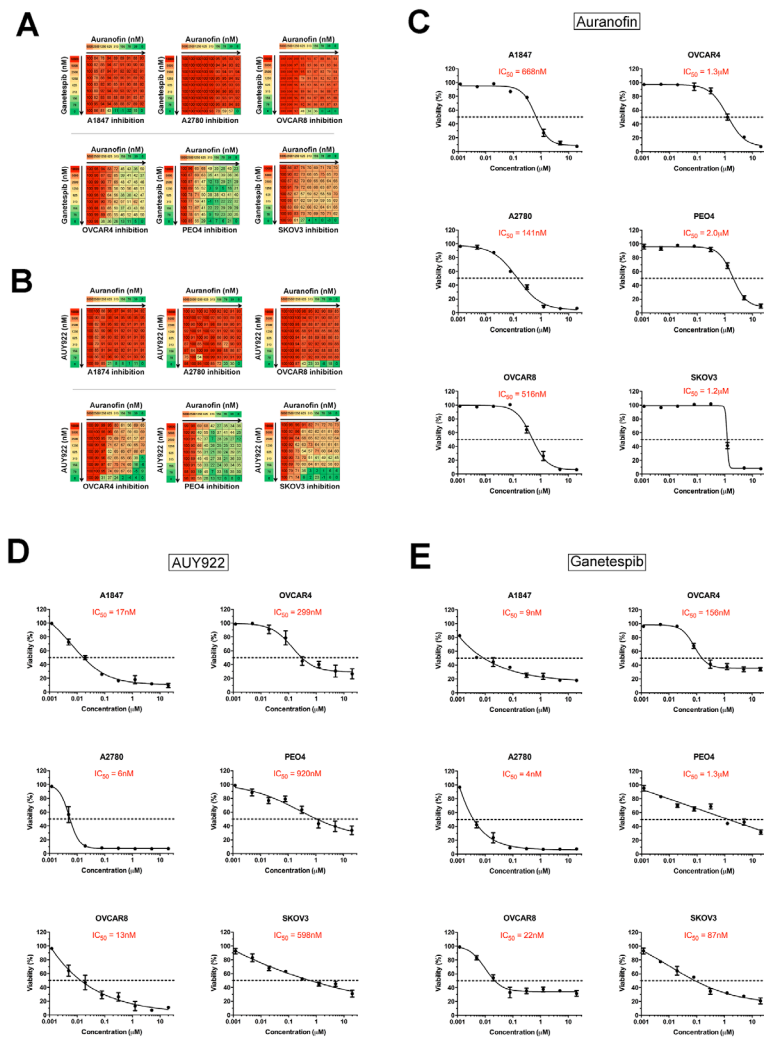
Cells in log phase of growth were grown to subconfluency, detached and seeded into 96-well plates at a concentration of 1×10^5 cells per well. Cells were allowed to attach overnight, washed then treated with or without compound at indicated concentrations and time points. Mitochondrial membrane potential was evaluated using the JC-1 Mitochondrial Membrane Potential Assay kit (Cayman Chemical) according to manufacturer protocol. Briefly, cells were exposed to JC-1 Staining Solution and incubated for 20 minutes at 37°C. The ratio of fluorescent intensity of J-aggregates to monomers was used as an indicator of mitochondrial membrane potential.

RT-qPCR primers

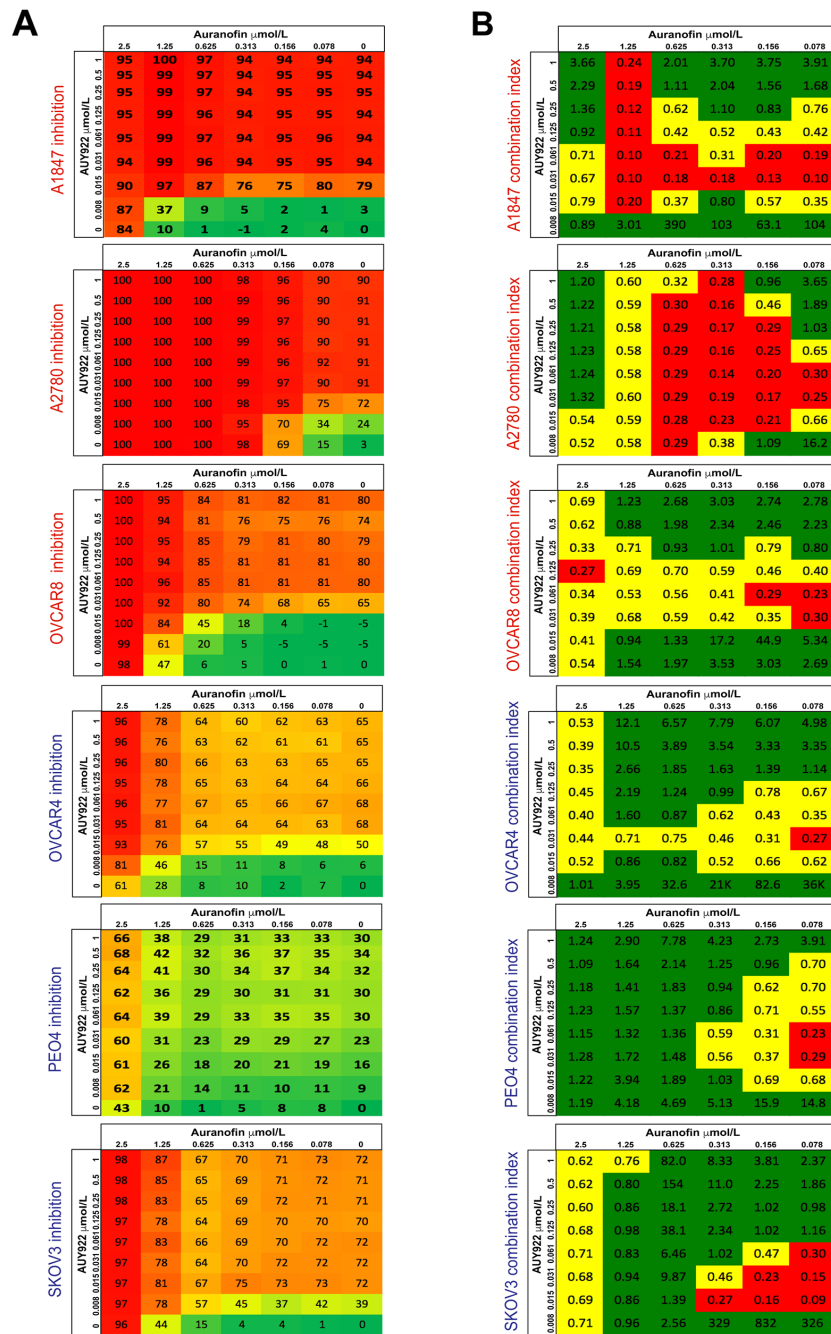
The following primers were used with SYBR® Green RT-PCR: Qiagen RT2 qPCR Primer Assay for Human TXN, PPH18986-200; Qiagen RT2 qPCR Primer Assay for Human TXNRD1, PPH02104F-200; Qiagen RT2 qPCR Primer Assay for Human HSP90AA1, PPH163391B-200; Qiagen RT2 qPCR Primer Assay for Human HSP90AB1, PPH01201C-200; IDT CDH6, GGAGGACAGGGAACAGTATTT, GAGCCGATATG

CCCTCATT; IDT WNT7A, CACTGGTGCTGCTATGTCAA, AGTACCCTCCTCAGCAGAAA; IDT IGFBP7, GTACTTGAGCTGTGAGGTCATC, CACCCA GCCAGTTACTTCAT; IDT ELFN1, GCCCTG ACACACAACAGGAA, GGGTGTCCCTGTCCCAAACC; IDT ITPRIPL1, GCTCGGACAAGCATGGTCTA, GCCTCTGCATCGTCAGTGTT; IDT MME, CTGCTGAGGGGTCACGATTTTA, AGGACCGAG AGGCTGATCTC. IDT PPIA, AGACAAGGTCC CAAAGAC, ACCACCCTGACACATAAA.

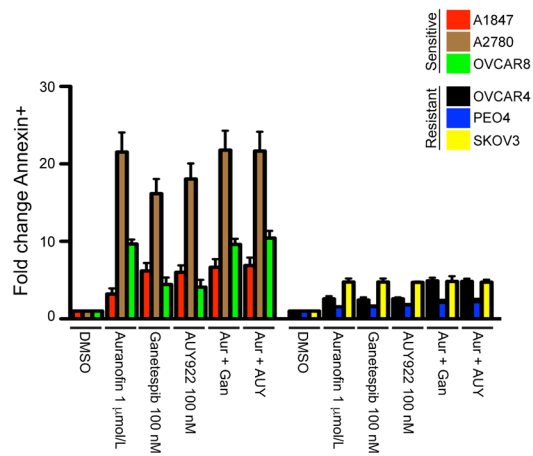
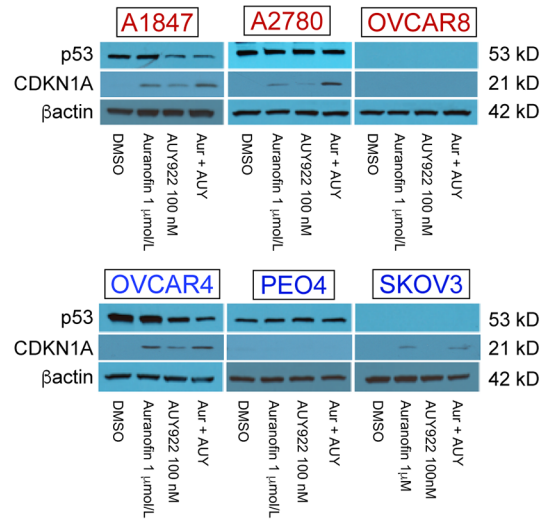
The following primers were used with TaqMan® RT-PCR: IGFBP7, Hs00266026_m1; KRT19, Hs01051611_gH; ESR1, Hs00174860_m1; MUC16, Hs01065189_m1; EHF, Hs00171917_m1; LAMA3, Hs00165042_m1; MMP2, Hs01548727_m1; CDH6, Hs01026780_m1; MXRA5, Hs01019147_m1; ITGB6, Hs00982345_m1; WNT7A, Hs00171699_m1; TACSTD2, Hs01922976_s1; S100A14, Hs04189107_g1; MAL2, Hs00294541_m1; ZBED2, Hs00976682_s1; IRF6, Hs01062178_m1; CACNA2D3, Hs01045015_m1; TSTD1, Hs00939899_g1; COL5A1, Hs00609133_m1; PDZK1IP1, Hs00173779_m1; FAT2, Hs01087225_m1; LAD1, Hs00194326_m1; CFI, Hs00989715_m1; GUSB, Hs00939627_m1; PPIA, Hs04194521_s1; TBP, Hs00427620_m1.



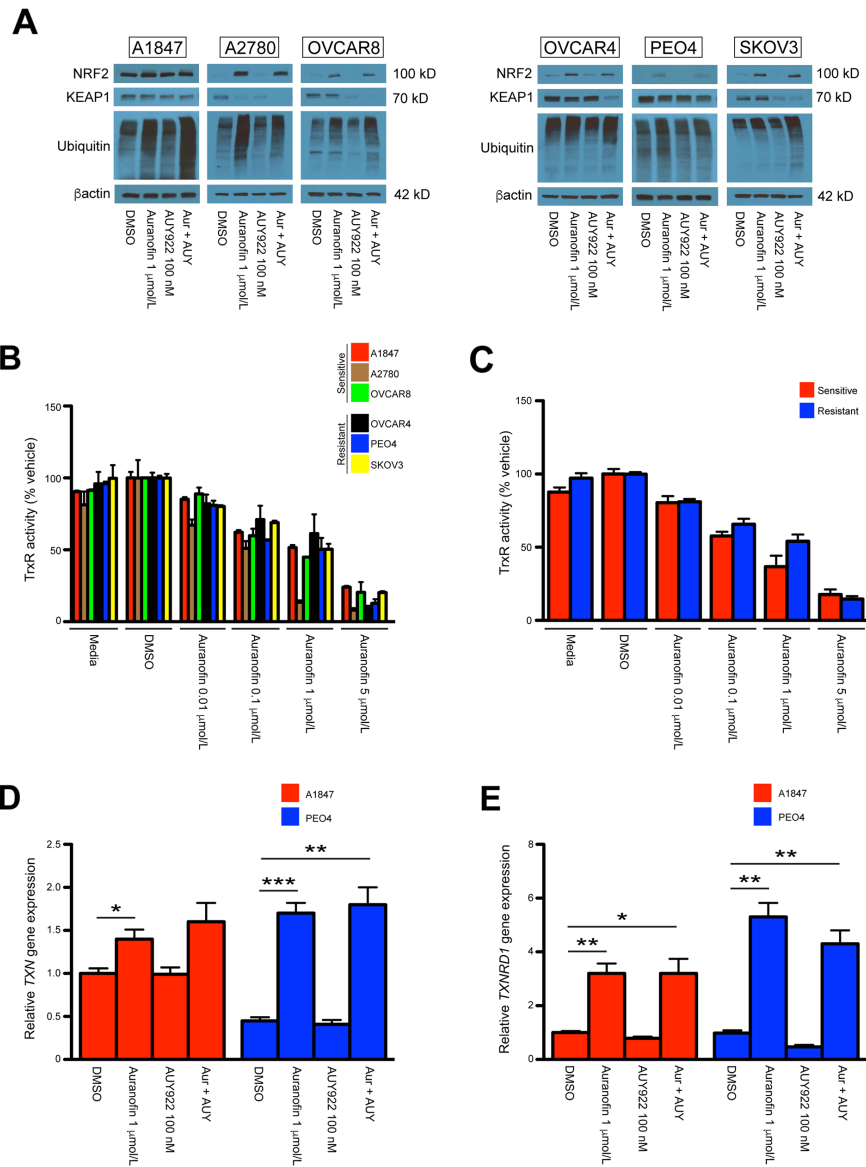
Supplementary Figure 1: Viability studies for auranofin and the HSP90 inhibitors AUY922 and ganetespib in sensitive and resistant cell lines. (A) Color scale for the percentage of viability inhibition is shown across 64 different drug combinations of auranofin and ganetespib for sensitive (upper) and resistant (lower) cell lines. (B) Color scale for the percentage of viability inhibition is shown across 64 different drug combinations of auranofin and AUY922 for sensitive (upper) and resistant (lower) cell lines. (C) IC_{50} values of auranofin treatment across six different EOC cell lines. The points represent average viability \pm standard error of mean following 72 hours of drug treatment at the indicated concentrations. Curve-fit lines were generated using non-linear regression analysis in GraphPad Prism. (D) IC_{50} values of AUY922 treatment across six different EOC cell lines. The points represent average viability \pm standard error of mean following 72 hours of drug treatment at the indicated concentrations. Curve-fit lines were generated using non-linear regression analysis in GraphPad Prism. (E) IC_{50} values of ganetespib treatment across six different EOC cell lines. The points represent average viability \pm standard error of mean following 72 hours of drug treatment at the indicated concentrations. Curve-fit lines were generated using non-linear regression analysis in GraphPad Prism.



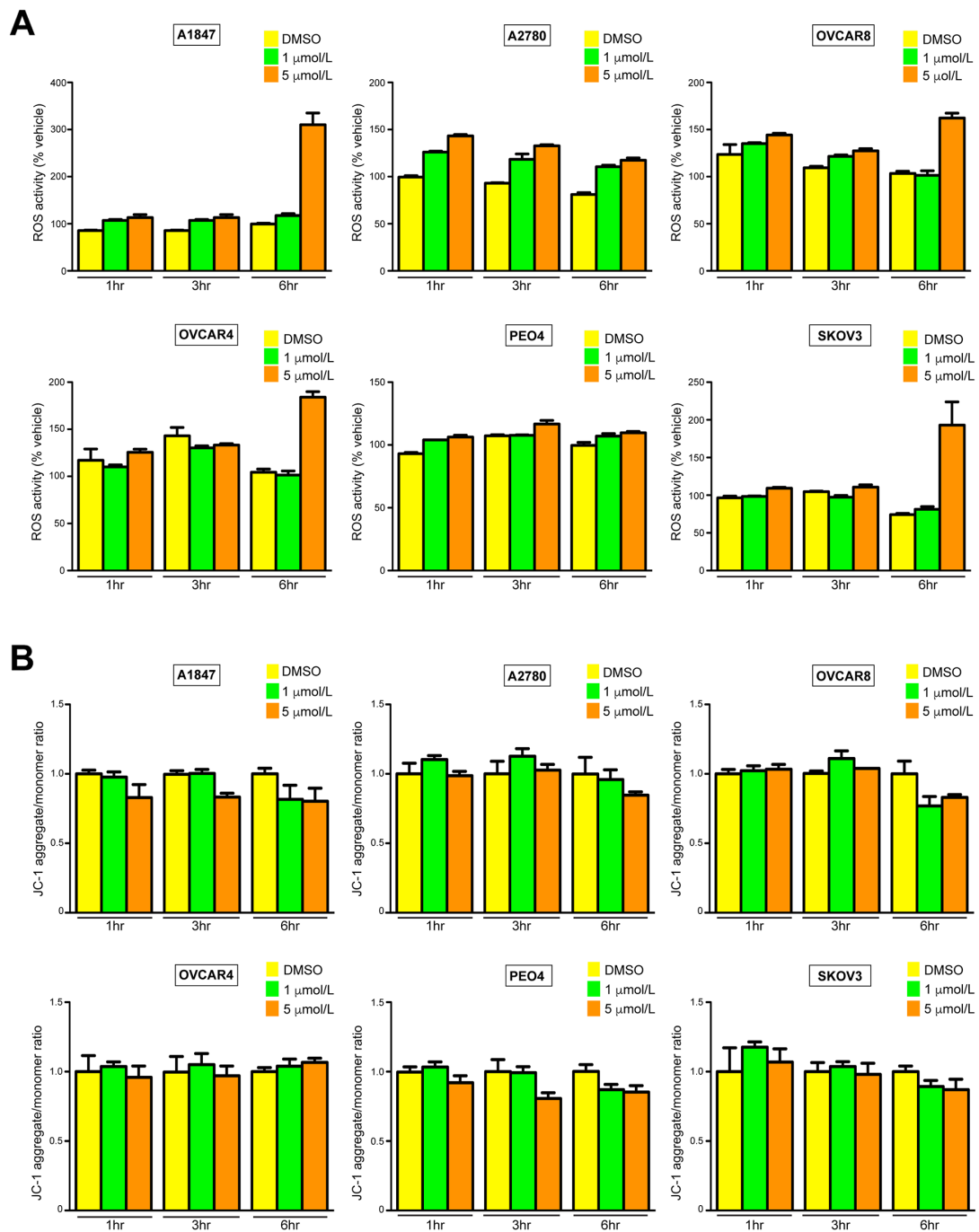
Supplementary Figure 2: Synergistic effects on of auranofin and AUY922 in sensitive and resistant cell lines. (A) Color scale for percentage of viability inhibition is shown across 48 different drug combinations of auranofin and AUY922 for sensitive (A1847, A2780, OVCAR8) and resistant (OVCAR4, PEO4, SKOV3) cell lines. **(B)** The dose response data was used to calculate the Combination index (CI) values for auranofin and AUY922 combination treatment for sensitive (A1847, A2780, OVCAR8) and resistant (OVCAR4, PEO4, SKOV3) cell lines. Shown is the average calculated CI value \pm standard error of the mean. CI value of >0.8 [green] indicates no synergy; CI = $0.3-0.8$ [yellow] indicates synergistic effects; CI value of <0.3 [red] indicates strong synergistic effects.

A**B**

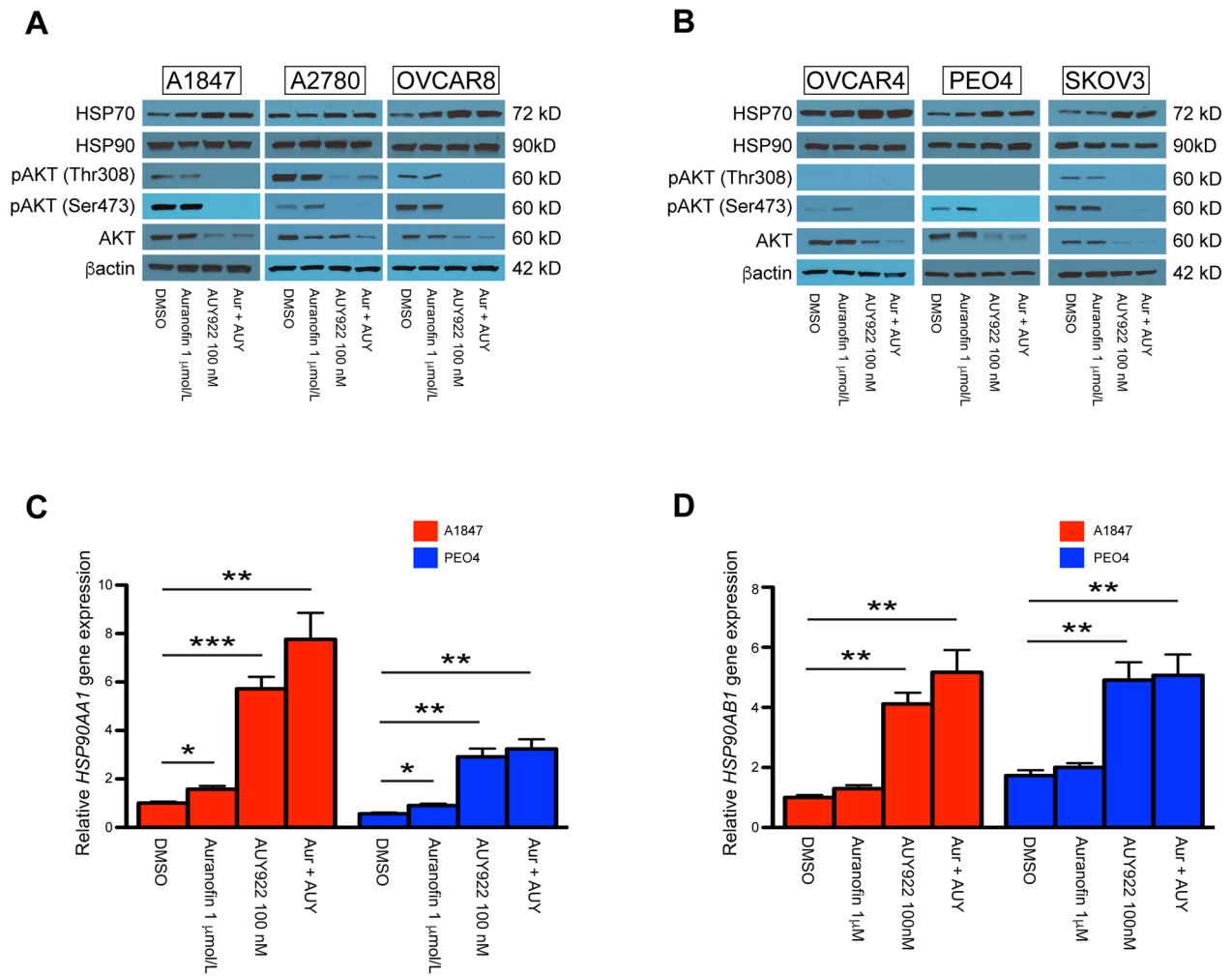
Supplementary Figure 3: Single agent and combinatorial effects of auranofin and AUY922 on apoptosis. (A) Fold-change of all sensitive and resistant cells positive for Annexin V staining 48 hours after incubation with indicated compounds, both alone and in combination (Aur + Gan and Aur + AUY). Data were quantified for the indicated fold-changes relative to vehicle treated cells and are presented as bar graphs showing the average fold-change \pm standard error of the mean. **(B)** Protein expression of TP53 and CDKN1A 24 hours after incubation with indicated compounds, both alone and in combination (Aur + AUY). β -actin was used as a loading control.



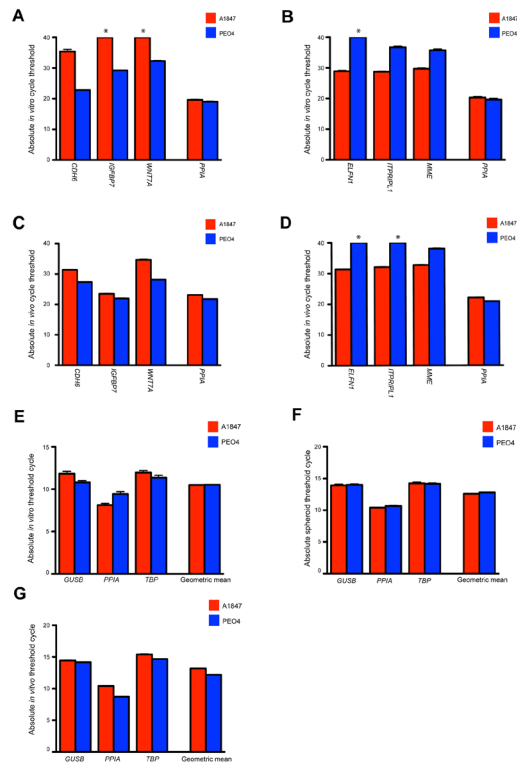
Supplementary Figure 4: Single agent and combinatorial effects of auranofin and AUY922 on reactive species homeostasis. (A) Protein expression of NRF2, KEAP1 and pan-ubiquitin 24 hours after incubation with indicated compounds, both alone and in combination (Aur + AUY). β -actin was used as a loading control. **(B)** Inhibition of TXNRD1 activity in sensitive (A1847, A2780, OVCAR8) and resistant (OVCAR4, PEO4, SKOV3) cell lines 6 hours after incubation with increasing concentrations of auranofin. **(C)** Collective inhibition of TXNRD1 activity in sensitive (A1847, A2780, OVCAR8) and resistant (OVCAR4, PEO4, SKOV3) cell lines 6 hours after incubation with increasing concentrations of auranofin. **(D, E)** Transcriptional expression of *TXN* and *TXNRD1* in A1847 and PEO4 cell lines 24 hours after incubation with the indicated compounds, both alone and in combination (Aur + AUY). Data were quantified for the indicated fold-changes relative to vehicle treated cells and are presented as bar graphs showing the average fold-change \pm standard error of the mean. * = $p < 0.05$, ** = $p < 0.01$, *** = $p < 0.001$.



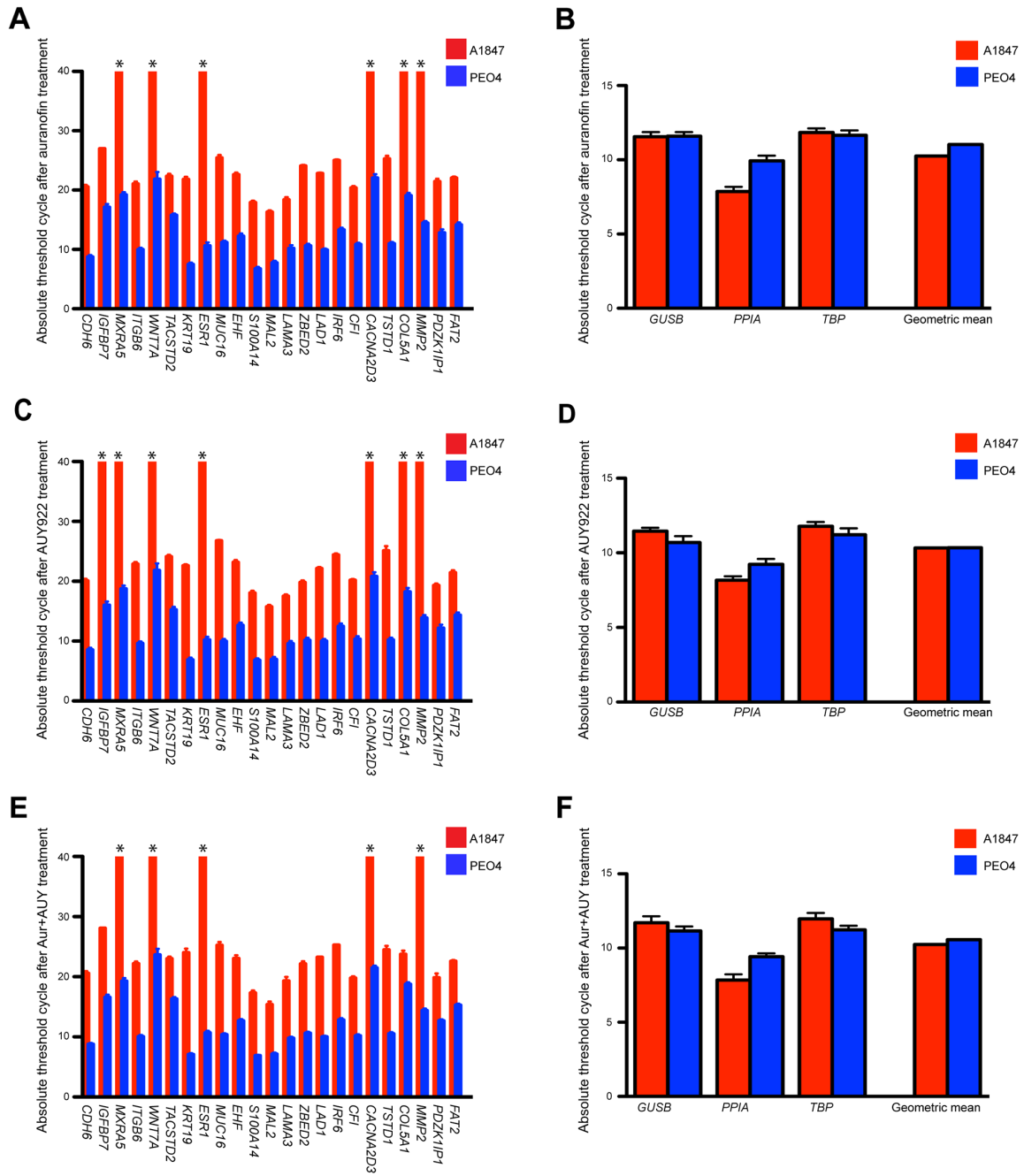
Supplementary Figure 5: Single agent effects of auranofin on reactive oxygen species homeostasis. (A) Measurement of ROS levels using DCF fluorescence after 6 hours auranofin treatment at the indicated concentrations for sensitive (A1847, A2780, OVCAR8) and resistant (OVCAR4, PEO4, SKOV3) cell lines. (B) Measurement of the JC-1 aggregate ratio after 6 hours auranofin treatment at the indicated concentrations for sensitive (A1847, A2780, OVCAR8) and resistant (OVCAR4, PEO4, SKOV3) cell lines. Data were quantified for the indicated fold-changes relative to vehicle treated cells and are presented as bar graphs showing the average fold-change \pm standard error of the mean.



Supplementary Figure 6: Single agent and combinatorial effects on the HSP90 pathway. (A, B) Protein expression of HSP70, HSP90, pAKT-Thr308, pAKT-Ser473 and AKT for sensitive (A1847, A2780, OVCAR8) and resistant (OVCAR4, PEO4, SKOV3) cell lines 24 hours after incubation with indicated compounds, both alone and in combination (Aur + AUJ). β -actin was used as a loading control. (C, D) Transcriptional expression of the *HSP90AA1* and *HSP90AB1* subunits in A1847 and PEO4 cell lines 24 hours after incubation with the indicated compounds, both alone and in combination (Aur + AUJ). Data were quantified for the indicated fold-changes relative to vehicle treated cells and are presented as bar graphs showing the average fold-change \pm standard error of the mean. * = $p < 0.05$, ** = $p < 0.01$, *** = $p < 0.001$.

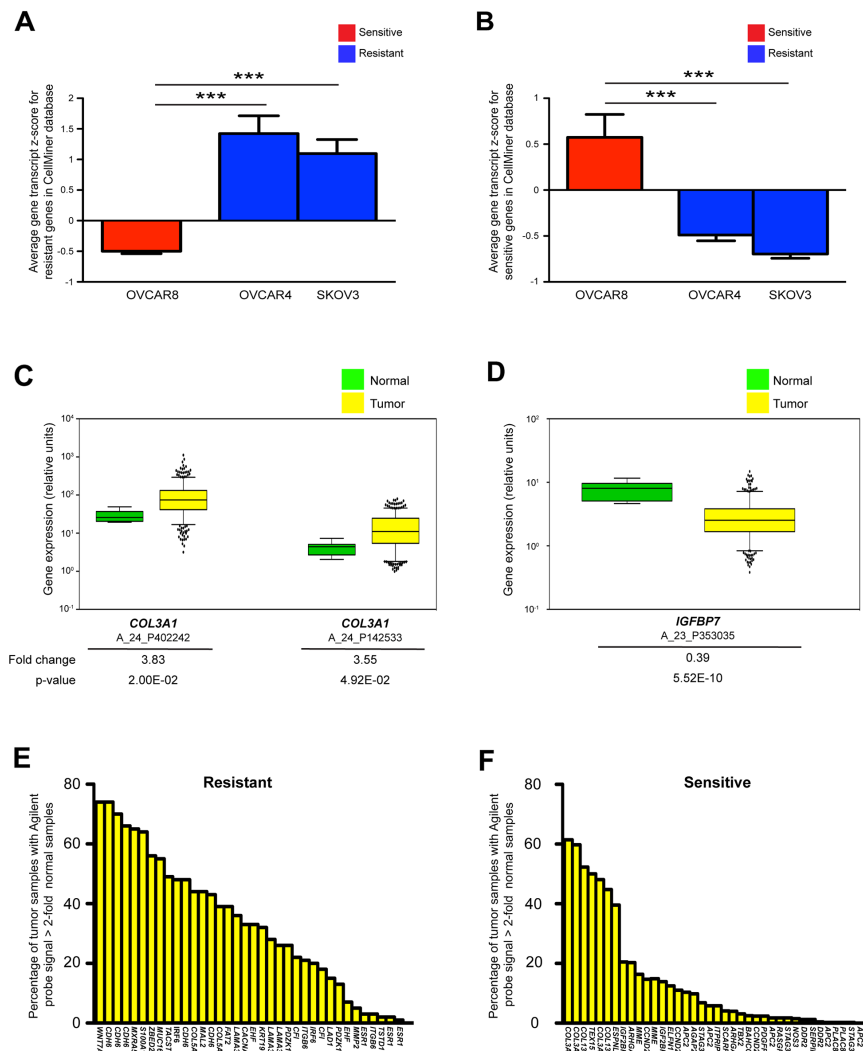


Supplementary Figure 7: Validation of genetic signature using real-time quantitative reverse transcription PCR. (A) Basal transcriptional expression of genes from the resistant genetic signature *CDH6*, *IGFBP7*, *WNT7A* and the reference control *PPIA* in A1847 and PEO4 cultured cells. Data are displayed as bar graphs representing the absolute threshold cycle \pm standard error of the mean from triplicate reactions of two independent experiments. Asterisks designate lack of amplification curves within 40 cycles. (B) Basal transcriptional expression of genes from the sensitive genetic signature *ELFN1*, *ITPRIPL1*, *MME* and the reference control *PPIA* in A1847 and PEO4 cultured cells. Data are displayed as bar graphs representing the absolute threshold cycle \pm standard error of the mean from triplicate reactions of two independent experiments. Asterisks designate lack of amplification curves within 40 cycles. (C) Basal transcriptional expression of genes from the resistant genetic signature *CDH6*, *IGFBP7*, *WNT7A* and the reference control *PPIA* in A1847 and PEO4 from *in vivo* xenografts. Data are displayed as bar graphs representing the absolute threshold cycle \pm standard error of the mean from triplicate reactions of two independent experiments. (D) Basal transcriptional expression of genes from the sensitive genetic signature *ELFN1*, *ITPRIPL1*, *MME* and the reference control *PPIA* in A1847 and PEO4 from *in vivo* xenografts. Data are displayed as bar graphs representing the absolute threshold cycle \pm standard error of the mean from triplicate reactions of two independent experiments. Asterisks designate lack of amplification curves within 40 cycles. (E-G) Three reference controls genes; *GUSB*, *PPIA* and *TBP* were evaluated along with their geometric mean using the Biomark high-density qPCR system utilizing TaqMan assays for the *in vitro*, spheroid formation and *in vivo* experiments, respectively. Average cycle threshold values \pm standard error of the mean from triplicate reactions of two independent experiments are graphed.

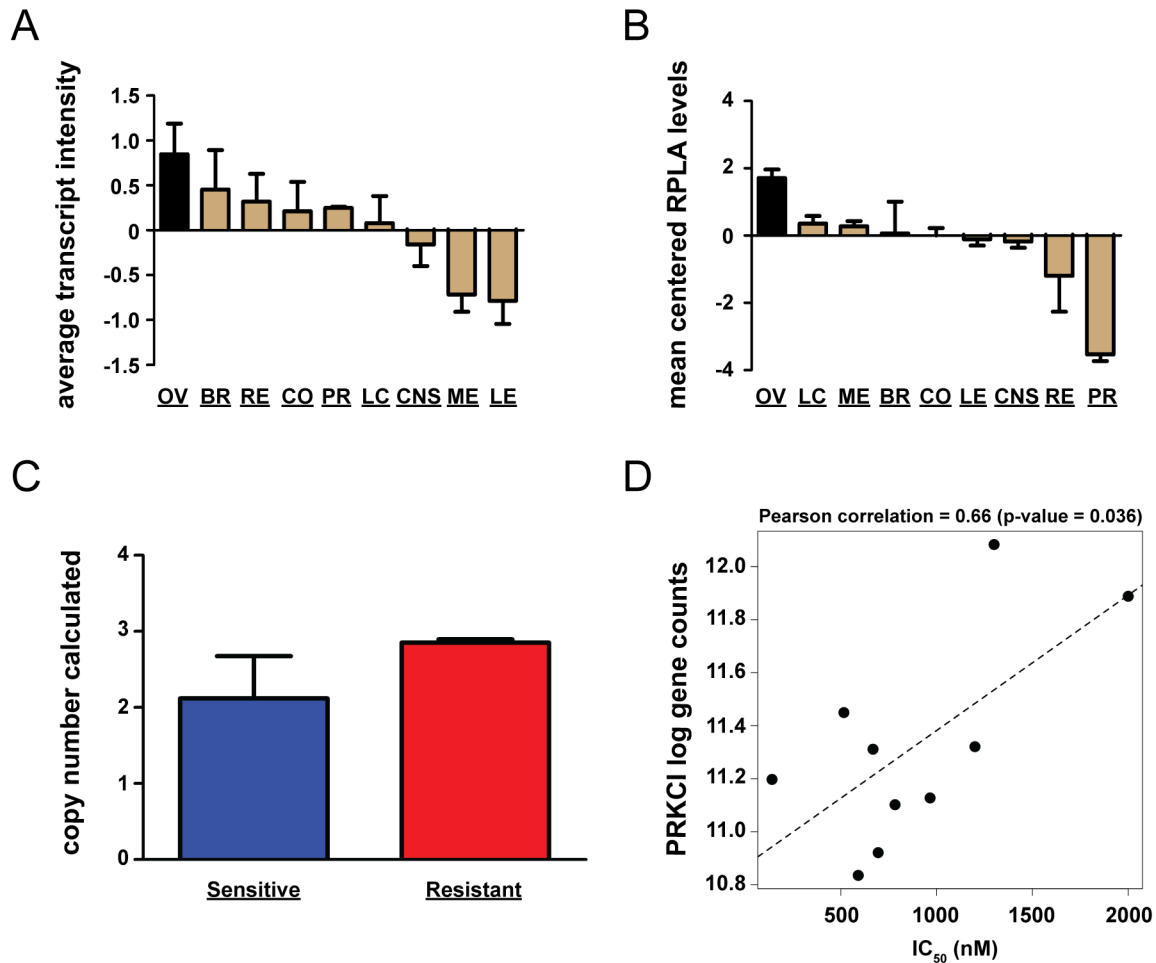


Supplementary Figure 8: Transcriptional variation of resistant signature after exposure to auranofin and AUY922.

(A, B) Transcriptional expression of 23 genes from the resistant genetic signature as well as three reference control genes; *GUSB*, *PPIA* and *TBP* alongside their geometric mean in A1847 and PEO4 cultured cells after incubation with 1 $\mu\text{mol/L}$ auranofin for six hours. (C, D) Transcriptional expression of 23 genes from the resistant genetic signature as well as three reference control genes; *GUSB*, *PPIA* and *TBP* alongside their geometric mean in A1847 and PEO4 cultured cells after incubation with 100 nM AUY922 for six hours. (E, F) Transcriptional expression of 23 genes from the resistant genetic signature as well as three reference control genes; *GUSB*, *PPIA* and *TBP* alongside their geometric mean in A1847 and PEO4 cultured cells after incubation with 1 $\mu\text{mol/L}$ auranofin and 100 nM AUY922 for six hours. Data are displayed as bar graphs representing the absolute threshold cycle \pm standard error of the mean from triplicate reactions of two independent experiments. Asterisks designate lack of amplification curves within 40 cycles.



Supplementary Figure 9: Investigation of publicly available datasets for prevalence of genetic signatures. (A, B) Average gene transcript z-score from the CellMiner dataset for resistant and sensitive genes from OVCAR8, OVCAR4 and SKOV3 cell lines. Data are displayed as bar graphs representing average z-scores \pm standard error of the mean. Positive and negative columns signify higher and lower z-scores, respectively. *** = $p < 0.001$. (C) Average expression values of Agilent probes related to an increase in the sensitive signature from 518 TCGA tumors relative to 8 fallopian control samples. Data are displayed as box plots representing 1 gene (derived from 2 unique probes) that showed average increase of expression in tumors (yellow) greater than 2-fold increase over fallopian (green). (D) Average expression values of Agilent probes related to a decrease in the resistant signature from 518 TCGA tumors relative to 8 fallopian control samples. Data is displayed as box plots representing 1 gene (derived from 1 unique probe) that showed average decrease of expression in tumors (yellow) greater than 2-fold increase over fallopian (green). The whiskers of each box plot represent expression values at 5th and 95th percentiles. Average fold change expression and p-values are indicated for each probe. (E, F) Percentage of 518 tumors in the ovarian TCGA dataset that express individual Agilent probes for the resistant and sensitive signature, respectively. Data are displayed as the percentage of tumors exhibiting single probe expression levels > 2-fold fallopian tissue for the same probe.



Supplementary Figure 10: PRKCI expression and copy number analysis using ovarian cell line models. (A, B) Average gene transcript z-score and protein RPLA levels from the CellMiner dataset for all lines within nine different human cancer types, respectively. Data are displayed as bar graphs representing average scores \pm standard error of the mean. Positive and negative columns signify higher and lower z-scores. OV-ovarian cancer, BR-breast cancer, RE-renal cancer, CO-colon cancer, PR-prostate cancer, LC-non small cell lung cancer, CNS-central nervous system, ME-melanoma, LE-leukemia. (C) Calculated copy number values for the sensitive (A1847, A2789, OVCAR8) and resistant (OVCAR4, PEO4, SKOV3) cell lines using CopyCaller® software. Data are displayed as bar graphs representing average scores \pm standard error of the mean. (D) PRKCI log gene counts versus IC₅₀ values of ten ovarian cell lines treated with auranofin. A Pearson coefficient was determined to measure linear correlation between the two variables, p-value < 0.05 is considered significant.

Supplementary Table 1 : List of cell lines and compounds used in preliminary high-throughput drug screen. Panel of 10 EOC cell lines utilized in a high-throughput drug screen encompassing 7 FDA-approved compounds and 12 different two-drug combinations.

Cell line	Description
A1847	untreated ovarian tumor
A2780	untreated ovarian tumor
C30	A2780 after intermittent exposure to cisplatin
CP70	A2780 after intermittent exposure to cisplatin
OVCAR4	ovarian tumor from a patient refractory to cisplatin
OVCAR5	untreated ovarian tumor (advanced)
OVCAR8	ovarian tumor from a carboplatin-refractory patient
OVCAR10	ovarian tumor from a cisplatin/carboplatin refractory patient
PEO4	ovarian tumor after patient became refractory
SKOV3	adenocarcinoma
Compound	Mechanism
Auranofin	reactive oxygen species inducer
Elesclomol	reactive oxygen species inducer
Bortezomib	26S proteasome inhibitor
Carfilzomib	20S proteasome inhibitor
Geldanamycin	ATP-binding pocket inhibitor
Ganetespib	ATP-binding pocket inhibitor
AUY922	Atp-binding pocket inhibitor

Supplementary Table 2 : Quantification of isoforms utilized in construction of the resistant signature. Expression of variant transcripts for genes related to resistance were compiled and quantified for the six cell lines. Data also display total average number of transcripts detected for each cell line as well as group averages per RefSeq ID.

Gene ID	RefSeq ID	A1847	A2780	OVCAR8	Average	OVCAR4	PEO4	SKOV3	Average
CDH6	NM_004932.3	8	12	2	7	9361	3567	7167	6698
IGFBP7	NM_001253835.1	0	0	1	0	22	6	34	21
IGFBP7	NM_001553.2	0	0	0	0	2695	494	3637	2275
MXRA5	NM_015419.3	0	0	0	0	2682	243	1957	1627
ITGB6	NM_000888.3	0	1	1	1	1075	2005	431	1170
WNT7A	NM_004625.3	0	1	0	0	2845	213	1338	1465
TACSTD2	NM_002353.2	24	0	7	10	5501	14808	2020	7443
KRT19	NM_002276.4	9	22	3	11	9757	9349	350	6485
ESR1	NM_000125.3	0	0	0	0	0	188	659	282
ESR1	NM_001122740.1	0	0	0	0	0	618	121	246
ESR1	NM_001122741.1	0	0	0	0	36	1039	493	523
ESR1	NM_001122742.1	0	0	0	0	0	0	0	0
MUC16	NM_024690.2	1	4	3	3	9897	14583	28	8169
EHF	NM_001206615.1	0	0	1	0	45	19	11	25
EHF	NM_001206616.1	0	0	0	0	0	0	72	24
EHF	NM_012153.5	0	1	0	0	996	354	198	516
S100A14	NM_020672.2	3	3	5	4	3336	3422	25	2261
MAL2	NM_052886.2	41	4	15	20	5604	15787	1066	7486
LAMA3	NM_000227.3	28	0	6	11	12834	7880	1347	7354
LAMA3	NM_001127717.1	0	0	0	0	0	0	0	0
LAMA3	NM_001127718.1	0	1	0	0	0	0	0	0
LAMA3	NM_198129.1	19	0	49	23	425	218	472	371
ZBED2	NM_024508.4	1	0	1	1	79	717	642	479
LAD1	NM_005558.3	1	9	0	3	4063	978	37	1693
IRF6	NM_001206696.1	0	1	0	0	192	34	0	76
IRF6	NM_006147.3	0	0	0	0	653	307	47	335
CFI	NM_000204.3	1	0	1	1	72	1159	191	474
CACNA2D3	NM_018398.2	0	0	0	0	209	64	144	139
TSTD1	NM_001113205.1	0	0	0	0	46	8	2	18
TSTD1	NM_001113206.1	0	0	0	0	96	31	19	49
TSTD1	NM_001113207.1	0	0	0	0	230	72	27	110
COL5A1	NM_000093.3	3	34	13	17	62	1053	23741	8285
MMP2	NM_001127891.1	0	4	0	1	29	0	0	10

(Continued)

Gene ID	RefSeq ID	A1847	A2780	OVCAR8	Average	OVCAR4	PEO4	SKOV3	Average
MMP2	NM_004530.4	0	0	2	1	0	796	1153	650
PDZK1IP1	NM_005764.3	0	0	1	0	79	247	227	184
FAT2	NM_001447.2	22	20	10	17	11481	523	35	4013
Average		4	3	3		2345	2244	1325	

Supplementary Table 3 : Quantification of isoforms utilized in construction of the sensitive signature. Expression of variant transcripts for genes related to sensitivity were compiled and quantified for the six cell lines. Data also display total average number of transcripts detected for each cell line as well as group averages per RefSeq ID.

Gene ID	RefSeq ID	A1847	A2780	OVCAR8	Average	OVCAR4	PEO4	SKOV3	Average
AGAP2	NM_001122772.2	0	381	0	127	0	0	0	0
AGAP2	NM_014770.3	43	429	69	181	3	0	5	3
APC2	NM_005883.2	196	878	33	369	4	4	10	6
ARHGAP28	NM_001010000.2	147	2806	396	1116	1	21	18	13
BAHCC1	NM_001080519.2	435	2381	53	956	3	3	37	14
CCND2	NM_001759.3	15	18074	18	6036	3	1	2	2
COL13A1	NM_001130103.1	0	0	0	0	0	0	0	0
COL13A1	NM_080798.3	6	0	206	71	5	0	0	2
COL13A1	NM_080800.3	38	0	257	98	0	0	0	0
COL13A1	NM_080801.3	20	17	36	24	0	0	0	0
COL13A1	NM_080802.3	33	0	307	113	0	0	0	0
COL13A1	NM_080805.3	64	0	148	71	0	5	7	4
COL3A1	NM_000090.3	11	23906	63	7993	4	132	12	49
DDR2	NM_001014796.1	0	318	0	106	0	0	0	0
DDR2	NM_006182.2	24	4231	46	1434	13	9	37	20
ELFN1	NM_001128636.2	105	2177	77	786	2	0	0	1
ESPNL	NM_194312.2	150	371	19	180	1	5	1	2
FREM2	NM_207361.4	229	4143	192	1521	2	48	1	17
IGF2BP1	NM_001160423.1	0	27	0	9	0	3	0	1
IGF2BP1	NM_006546.3	3623	14860	152	6212	25	0	2	9
ITPRIPL1	NM_001008949.2	150	172	106	143	0	0	0	0
ITPRIPL1	NM_001163523.1	24	310	69	134	1	0	0	0
ITPRIPL1	NM_001163524.1	35	1	0	12	0	0	1	0
ITPRIPL1	NM_178495.5	12	0	0	4	0	0	0	0
MME	NM_000902.3	122	26	147	98	0	9	0	3
MME	NM_007287.2	279	0	216	165	2	0	8	3
MME	NM_007288.2	27	0	0	9	0	0	0	0
MME	NM_007289.2	45	0	0	15	0	0	0	0

(Continued)

Gene ID	RefSeq ID	A1847	A2780	OVCAR8	Average	OVCAR4	PEO4	SKOV3	Average
NOS3	NM_000603.4	222	858	277	452	8	11	19	13
NOS3	NM_001160109.1	0	0	0	0	0	0	0	0
NOS3	NM_001160110.1	0	2	0	1	0	0	0	0
NOS3	NM_001160111.1	2	0	0	1	0	0	0	0
PDGFRB	NM_002609.3	422	676	334	477	1	1	39	14
PLAC8	NM_001130715.1	2	0	0	1	0	0	0	0
PLAC8	NM_001130716.1	65	0	37	34	41	0	21	20
PLAC8	NM_016619.2	3626	59	3231	2306	0	13	47	20
RASGRP2	NM_001098670.1	0	60	0	20	0	1	0	0
RASGRP2	NM_001098671.1	44	37	0	27	0	0	0	0
RASGRP2	NM_153819.1	0	83	33	39	0	0	0	0
SCARF1	NM_003693.2	21	13	307	114	0	0	0	0
SCARF1	NM_145350.1	0	0	35	12	0	0	0	0
SCARF1	NM_145352.2	17	7	0	8	2	6	1	3
SCARF1	NR_028075.1	0	0	0	0	0	0	0	0
SCARF1	NR_028076.1	13	6	32	17	0	0	0	0
SERPINF1	NM_002615.5	25	2867	39	977	5	3	2	3
STAG3	NM_012447.2	2811	34	1	948	23	7	6	12
TBX2	NM_005994.3	42	11520	65	3876	16	10	37	21
TEX15	NM_031271.3	72	3782	38	1297	1	14	1	5
Average		275	1990	147		3	6	7	

Supplementary Table 4 : List of lncRNAs upregulated in sensitive and resistant panels. lncRNA sequencing analyses was condensed to Gene ID, Gene name, logFC (log2-fold change) and FDR (Benjamini-Hochberg adjusted p-value to account for multiple comparisons). The lists of lncRNAs that exhibit the highest logFC and FDR in the three sensitive cell lines as well as those from the three resistant lines are shown

SENSITIVE LINES			
Gene ID	Gene name	logFC	FDR
HOTAIR	HOX transcript antisense RNA	8.4	0.013
LINC02381	Long intergenic non-protein coding RNA 2381	5.9	0.039
AFAP1-AS1	AFAP1 antisense RNA 1	6.8	0.039
RESISTANT LINES			
Gene ID	Gene name	logFC	FDR
LINC02167	Long intergenic non-protein coding RNA 2167	11.7	0.005
EMX2OS	EMX2 opposite strand/ antisense RNA	7.7	0.007

(Continued)

RESISTANT LINES			
Gene ID	Gene name	logFC	FDR
LINC01559	Long intergenic non-protein coding RNA 1559	9.2	0.013
FLJ22447	Uncharacterized LOC400221	5.3	0.013
ZNF625-ZNF20	ZNF625-ZNF20 readthrough (NMD candidate)	7.5	0.024
C8orf34-AS1	C8orf34 antisense RNA 1	9.3	0.039

Supplementary Table 5 : List of cycle threshold variations of the resistant genetic signature related to auranofin and AUY922. Absolute cycle threshold variation of 23 genes from the resistant signature in A1847 and PEO4 cultured cells treated with the indicated compounds, both alone and in combination (Aur + AUY). Data represent the difference of absolute threshold cycle \pm standard error of the mean as compared to basal transcription from triplicate reactions of two independent experiments. Positive and negative numbers signify higher and lower Ct values, respectively

Gene ID	Auranofin A1847	Auranofin PEO4	AUY922 A1847	AUY922 PEO4	Aur + AUY A1847	Aur + AUY PEO4
CDH6	-0.7	1.2	-1.1	-0.2	-0.7	0.1
IGFBP7	NA	0.3	NA	0.1	NA	0.6
MXRA5	NA	0.9	NA	-0.1	NA	0.4
ITGB6	-0.2	0.3	1.6	0.6	0.9	1.0
WNT7A	NA	0.8	NA	0.3	NA	2.1
TACSTD2	-1.5	0.6	0.3	0.3	-0.8	1.4
KRT19	-1.6	0.4	-0.8	0.1	0.6	0.3
ESR1	NA	1.0	NA	0.0	NA	0.4
MUC16	1.2	-0.4	2.6	-0.2	1.0	0.2
EHF	-2.0	-0.2	-1.4	-0.1	-1.5	0.0
S100A14	-0.2	0.7	0.0	-0.2	-0.8	-0.1
MAL2	-0.7	1.3	-1.2	-0.1	-1.6	0.1
LAMA3	0.3	0.3	-0.5	0.7	1.3	0.9
ZBED2	3.3	0.2	-1.0	-0.1	1.3	0.3
LAD1	-2.1	0.6	-2.7	0.3	-1.6	0.3
IRF6	1.1	0.7	0.5	-0.2	1.3	0.1
CFI	0.3	1.2	0.2	0.2	-0.3	0.1
CACNA2D3	NA	0.5	NA	0.0	NA	0.7
TSTD1	> -15.7	0.8	> -15.9	-0.2	> -16.5	0.1
COL5A1	NA	0.6	NA	0.0	> -17.2	0.5
MMP2	NA	0.6	NA	0.0	NA	0.5
PDZK1IP1	1.1	0.0	-1.0	-0.6	-0.5	-0.1
FAT2	0.7	0.3	0.1	0.5	1.2	1.4

Supplementary Table 6: List of Agilent probes from the ovarian TCGA tumor dataset demonstrating increased and decreased expression of signature genes as compared to normal tissue. Agilent gene expression data from TCGA on 518 serous adenocarcinomas and 8 fallopian tube samples derived from healthy individuals were queried for the two sets of 23 signature genes. Nine Agilent probes from the resistant signature showed ≥ 2 -fold increase in the average gene expression of its respective genes in the tumor samples relative to controls. Two Agilent probes from the sensitive signature showed ≥ 2 -fold increase in the average gene expression of its respective genes in the tumor samples relative to controls. One Agilent probe from the resistant signature showed ≥ 2 -fold increase in the average gene expression of its respective gene in the control samples relative to tumors. Seven Agilent probes from the sensitive signature showed ≥ 2 -fold increase in the average gene expression of its respective gene in the control samples relative to tumors. Data from multiple probes shown when available. The p-values were calculated using an unpaired two-tailed t-test using GraphPad Prism.

Increased expression of Resistant signature genes in TCGA tumor samples							
Gene ID	Agilent Probe ID	Normal Expression	SEM	Tumor Expression	SEM	Fold Change	p value
CDH6	A_24_P687	2.41	0.28	7.242	0.21	3.00	3.85E-03
IRF6	A_23_P748	5.36	0.51	11.417	0.26	2.13	4.53E-03
MXRA5	A_23_P258136	2.25	0.48	7.560	0.24	3.36	6.08E-03
WNT7A	A_23_P258410	1.74	0.14	12.346	0.52	7.08	1.21E-02
MUC16	A_23_P5211	3.98	0.86	10.417	0.33	2.62	1.59E-02
CDH6	A_23_P214011	4.76	0.78	29.476	1.32	6.19	2.02E-02
MAL2	A_23_P60130	3.30	0.24	7.050	0.20	2.13	2.21E-02
ZBED2	A_23_P113793	25.76	4.32	73.089	2.74	2.84	3.24E-02
S100A14	A_23_P124619	0.63	0.10	2.377	0.11	3.80	4.97E-02
Decreased expression of Resistant signature genes in TCGA tumor samples							
Gene ID	Agilent Probe ID	Normal Expression	SEM	Tumor Expression	SEM	Fold Change	p value
IGFBP7	A_23_P353035	7.75	0.87	3.05	0.09	0.39	5.52E-10
Increased expression of Sensitive signature genes in TCGA tumor samples							
Gene ID	Agilent Probe ID	Normal Expression	SEM	Tumor Expression	SEM	Fold Change	p value
COL3A1	A_24_P402242	4.24	0.59	16.28	0.64	3.83	0.02
COL3A1	A_23_P142533	29.51	3.69	104.83	4.80	3.55	0.05
Decreased expression of Sensitive signature genes in TCGA tumor samples							
Gene ID	Agilent Probe ID	Normal Expression	SEM	Tumor Expression	SEM	Fold Change	p value
PLAC8	A_24_P183128	1.43	0.25	0.16	0.01	0.11	8.41E-33
STAG3	A_23_P145657	3.27	0.51	0.58	0.03	3.55	5.36E-27
DDR2	A_32_P88965	1.19	0.24	0.53	0.02	0.44	3.40E-05
SERPINF1	A_23_P100660	1.67	0.26	0.76	0.03	0.45	4.63E-04
BAHCC1	A_23_P49539	0.53	0.04	0.25	0.01	0.47	0.003
CCND2	A_24_P278747	1.46	0.12	0.59	0.03	0.41	0.001
TBX2	A_23_P164451	2.66	0.27	1.13	0.07	0.43	0.01